Microneedle-based precision payload delivery in plants

Mingzhuo Li[1], Aditi Dey Poonam[1], Deepjyoti Singh[2], Anna Whitfield[2,3], and Qingshan Wei[1,3] *

1. Department of Chemical and Biomolecular Engineering, North Carolina State University, Raleigh, NC 27695
2. Department of Entomology and Plant Pathology, North Carolina State University, Raleigh, NC, 27606
3. Emerging Plant Disease and Global Food Security cluster, North Carolina State University, Raleigh, NC 27695

* Corresponding email: qwei3@ncsu.edu

Running title: **Precision molecular delivery to live plants with microneedles**

Keywords: plant delivery, microneedle, phytohormone, pathogen resistance, precision agriculture

Abstract:

Traditional crop delivery methods, such as foliar spray and soil application, face significant limitations including nutrient loss, environmental impacts, and low delivery efficiency. Recent advances in nanomaterials have offered novel molecular delivery platforms, but challenges such as toxicity, complexity, and labor-intensive processes persist. To address these issues, we developed a polyvinyl alcohol (PVA)-based microneedle (MN) delivery system that can be precisely applied to various plant tissues (e.g., leaves or stems), which demonstrates high delivery efficiency compared to the conventional methods while reducing application dose by 90-99%. This MN system facilitates delivery of diverse small molecules ranging from fluorescent dyes, growth promoters, to antiviral agents into plant tissues. By applying fluorescent dye-loaded MNs onto tomato stems, we demonstrated effective molecular diffusion through vascular tissues. Additionally, MNs loaded with gibberellic acid (GA3) enhanced stem and branch growth in tomatoes and restored the lateral flowering phenotype in *Arabidopsis ft-10* mutants, with significant upregulation of GA receptor gene expression. Lastly, salicylic acid (SA) injections with MNs induced resistance to Tomato Spotted Wilt Virus (TSWV) in *Nicotiana Benthamiana*, comparable to conventional spray-based approaches. This easily fabricated and cost-effective PVA-MN system provides a promising tool for precision agriculture, enhancing plant health and productivity while addressing the limitations of conventional delivery methods.

Keywords: plant delivery, microneedle, phytohormone, pathogen resistance, precision agriculture

53 **Introduction:**

54 Currently, two of the most widely used methods for active delivery in agriculture are foliar spray
55 and soil application (Niu *et al.*, 2021, Nkebiwe *et al.*, 2016). These two methods are popular due
56 to their simplicity, speed, and ease of scaling up. However, with the ongoing development of the
57 agricultural industry, significant limitations of these traditional delivery methods have become
58 apparent (Sinha *et al.*, 2022, Zheng *et al.*, 2020). As larger areas of cropland and a wider variety
59 of crops are integrated into the agricultural industry to meet the increasing food demands driven
60 by rapid population growth, these methods face new challenges (Davis *et al.*, 2016, Fukase &
61 Martin, 2020).

62 The first limitation is nutrient loss. In the foliar spray method, as much as 70% of the
63 chemicals are lost during the application process (Niu et al., 2021, Ishfaq *et al.*, 2022). While the
64 soil application saves more chemicals or nutrients, it still has nearly 10% to 30% lost in this method
65 (Pahalvi *et al.*, 2021, Yahaya *et al.*, 2023), due to numerous factors such as leaching, runoff, or
66 volatilization. Another major limitation is the impact of environment. In the foliar spray methods,
67 most of the chemicals may quickly run off into the atmosphere (Niu et al., 2021, Tyagi *et al.*, 2022),
68 or be washed away by rain, leading to environmental pollutions. On the other side, the large
69 amount of chemicals applied into the soil would bring lots of problems including water
70 contamination, soil pH value change, soil degradation, and finally results in negative impacts to
71 biodiversity in the soil (Young *et al.*, 2021, Brichi *et al.*, 2023, Alkharabsheh *et al.*, 2021). Finally,
72 foliar spray is a low-efficiency delivery method because the leaf cuticles act as a strong barrier that
73 slows down the nutrient and chemical absorption (Krishnasree *et al.*, 2021, Vasundhara & Chhabra,
74 2021, Barłóg *et al.*, 2022). This method also often provides only short-term relief from nutrient
75 deficiencies and needs to be repeated more frequently. Similarly, soil applications are low efficient
76 because of the slow plant responses, as the nutrients need to move through the soil profile before
77 being absorbed by the roots (Barłóg et al., 2022, Dimkpa *et al.*, 2020).

78 In recent years, several approaches have been developed to address those limitations in
79 traditional crop delivery systems to make molecular delivery in plants more effective, optimize
80 resource utilization, and minimize environmental impact. One example is the wide trials of using
81 nanomaterials in plant delivery systems (Salama *et al.*, 2021, Liu *et al.*, 2021, Jakhar *et al.*, 2022,
82 Beig *et al.*, 2022). Nanomaterials show characteristics that protect labile compounds from fast

83 degradation, increase the adhesion of payloads to plants, control the release of payloads, and
84 enhance the permeability of payloads through cuticles or internalization into plant tissues or cells
85 (Nair *et al.*, 2010, Cunningham *et al.*, 2018). For example, nanocarriers (e.g., carbon nanotubes,
86 quantum dots, and metal/metal oxide NPs) are designed to delivery DNA molecules to perform
87 plant genome engineering, such as gene transformation, si-RNA silencing, and gene editing
88 (Cunningham et al., 2018, Nair et al., 2010, Wang *et al.*, 2021, Zhang *et al.*, 2021, Zhang *et al.*,
89 2022, Zhang *et al.*, 2020). However, most of these genetic molecular delivery methods based on
90 the nanoparticles are limited by the complex nanomaterials design. In addition, toxicity of
91 nanoparticles to plants and animals is still a big concern (Cunningham et al., 2018). Furthermore,
92 these methods are also commonly applied by spraying, which suffer from the method-associated
93 low uptake efficiency (~0.1% for root application and <30% via leaf) (Tudi *et al.*, 2021).
94 Alternative delivery methods such as foliar infiltration are labor-intensive and leaf-restricted,
95 limiting their use in the field and for broad plant species.

96 The microneedle (MN) is a new technique that has been applied to precision agricultural
97 activities recently (Jung & Jin, 2021, Nagarkar *et al.*, 2020). MN refers to microscopic needles,
98 typically ranging from 150 to 1500 μm in length, 50 to 250 μm in base width and 1 to 25 μm in tip
99 diameter. MNs can be applied to plant tissues to enhance the delivery of essential compounds such
100 as nutrients, metabolites, and agrochemicals, thereby improving plant health and productivity
101 (Faraji Rad, 2023, Ece *et al.*, 2023). A previous example of the MNs in plant delivery is
102 biocompatible silk MNs that were developed for precision delivery of pesticides and essential
103 compounds into plants (Cao *et al.*, 2023, Cao *et al.*, 2020, Han *et al.*, 2025). Even though this silk-
104 based MN provides a new tool to deliver physiologically functional compounds into crops, the
105 source of materials and fabrication process limit its wide applications in large-scale agricultural
106 activities.

107 In our previous study, we developed a different MN system using polyvinyl alcohol (PVA)
108 as the base material (Paul *et al.*, 2021, Paul *et al.*, 2020, Paul *et al.*, 2022). The PVA-based MN
109 effectively isolated genetic molecules (e.g., DNA and RNA) from plant tissues, demonstrating its
110 potential for use in early and in-field crop disease diagnostics (Paul et al., 2020, Paul et al., 2022).
111 More recently, we also applied PVA MNs to crop seeds (e.g., soybeans), and demonstrated its

capability for rapid seed DNA extraction for genotyping and whole genome sequencing, a much-simplified trait analysis technology that can greatly speed up the breeding process (Li *et al.*, 2025)

In this study, we explored the capability of cost-effective and easy-to-scale-up PVA-MN to deliver small molecules into plant systems. We first observed the diffusion of fluorescent dyes from MN needle tips into tomato stem vascular tissues. Then, we demonstrated the MN-assisted delivery of plant hormone gibberellic acid3 (GA3) to promote plant growth and restore lateral flowering in Arabidopsis ft-10 mutants. Finally, we tested the delivery of salicylic acid (SA) to model plant *Nicotiana Benthamiana* to inhibit the transportation of tomato spotted wilt virus (TSWV). Together, these results demonstrated PVA-MN's effectiveness in delivering small molecules, particularly plant hormones, to plants. This PVA-MN system holds great promise for future applications in precision agriculture.

Results:

Delivery of fluorescent molecules in plant tissue

PVA (Polyvinyl Alcohol) is a synthetic polymer with several distinct characteristics, such as water solubility, biodegradability, non-toxicity, and tunable mechanical properties, making it a good candidate for applications in plant delivery. To test whether PVA-MN could be applied in chemical delivery in plant tissue, we first applied it to both the leaf and stem of tomato plants. Due to the strong hygroscopic nature of PVA, we observed that leaf tissues punctured by the PVA-MN dehydrated rapidly if the PVA-MN was not removed immediately (e.g., contact time >20 s) after penetration, causing surrounding tissues to wilt within an hour post-puncture (Figure S1). In contrast, when the MN was applied to the stem, although localized dehydration occurred at the puncture site, the vascular bundles remained largely unaffected and continued to function properly (Figure S1). These results indicate that the MN contact time for leaf delivery needs to be controlled, whereas the stem is a more robust delivery site for PVA MNs.

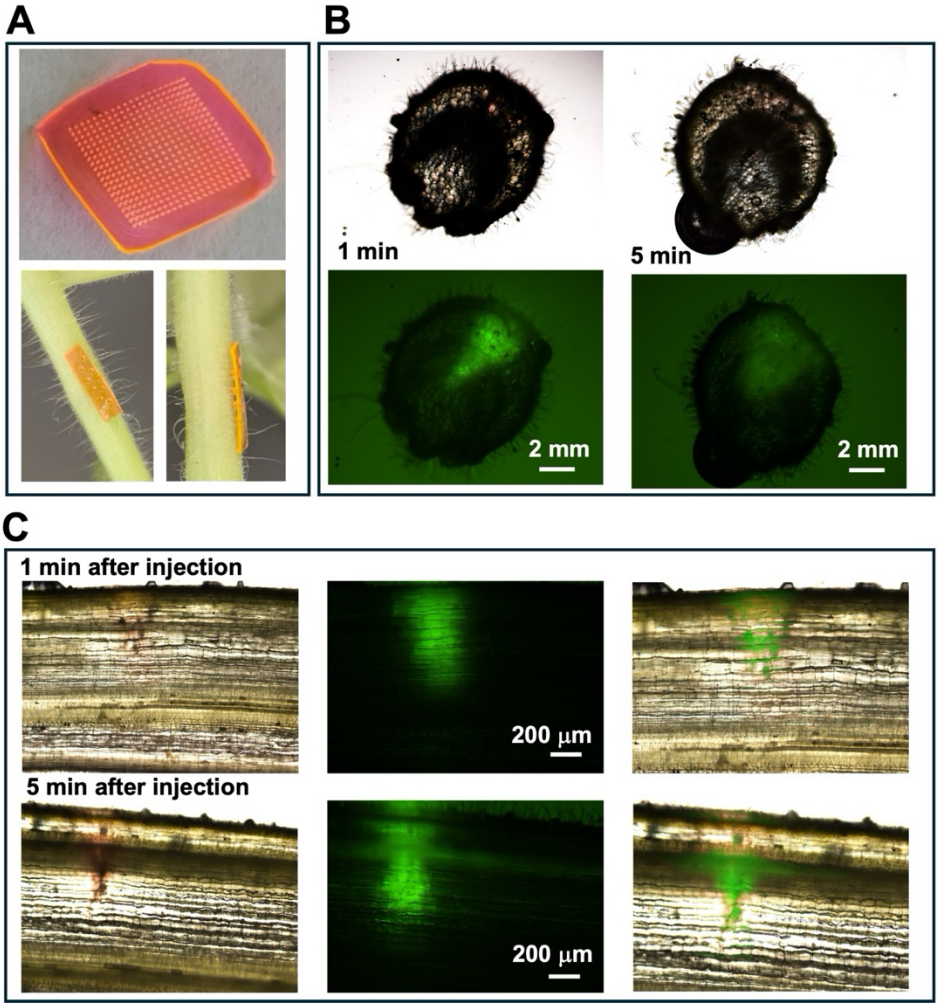

Fig. 1: PVA-MN delivery of fluorescent dyes to tomato plant vasculature system. A. Photographs of rhodamine 6G-loaded PVA MN (top) and a PVA patch loaded with 5(6)-carboxyfluorescein diacetate, inserted into tomato stem (bottom). B. Cross-section brightfield and fluorescence microscopy images of the injection site of PVA-MN, depicting that the needle reaches tomato's petiole vasculature system. The loaded dye diffuses out from the needle tip after 1 min and 5 mins of injection. C. Vertical-section microscopy images (from left to right: brightfield, fluorescence, and overlap) showing 5(6)-carboxyfluorescein diacetate delivered and transported along xylem, after 1min and 5 min of PVA needle injection.

Tomato was chosen as the model system due to its well-defined vasculature structure and long petioles. Previous studies have shown that the segment between the vasculature and the

151 epidermis ranges from 840–1040 μm for xylem and 707–925 μm for phloem in tomato plants, with
152 xylem and phloem diameters in the tens and hundreds of micrometers, respectively (Cao et al.,
153 2020). Based on these parameters, we designed and fabricated a 1000-μm-long PVA-MN as a
154 microinjector to study payload delivery in planta. We incorporated rhodamine 6G (maximum
155 absorption at 526 nm) and 5(6)-carboxyfluorescein diacetate (maximum absorption at 492 nm) as
156 dye markers into the PVA-MN (Figure 1A). The cross-sectional microscopic images of the petiole
157 confirmed that the 1000 μm MN reached the vascular tissues in the tomato stem (Figure 1B).

158 Using a GFP filter, we observed the diffusion of the 5(6)-carboxyfluorescein diacetate dye
159 into surrounding tissues within 5 minutes of PVA-MN injection (Figure 1B). To analyze molecular
160 transport in the xylem, we performed tangential sectioning of the stem and monitored the dye
161 diffusion at 1-, 5-, and 10-minutes post-injection by fluorescence imaging. The results showed
162 significantly more widespread distribution at 5 minutes post-injection compared to 1 minute
163 (Figure 1C). Quantification of relative fluorescence intensity showed a 32% and 77% increase of
164 dye diffusion area in stems at 5- and 10-minute post-injection, respectively (Figure S2).
165 Additionally, the chemical dyes were observed to travel along the xylem flow in the tomato stem
166 (Figure S3). These findings strongly suggest that the PVA-MN tip effectively reaches the
167 vasculature and that chemical compounds embedded in the PVA-MN can diffuse and be
168 transported along the vascular bundle delivery system in tomato plants.

169

170 **Delivery of growth regulator GA3 to promote tomato plant growth**

171 To demonstrate the utility of PVA-MN to deliver PGRs (Plant Growth Regulators) in crops, we
172 investigated the delivery of gibberellic acid (GA3) to vegetable tomato plants. GA3 is a plant
173 hormone that plays a crucial role in regulating various growth and developmental processes in
174 plants, such as seed germination, stem elongation, flowering, and fruit development (Gupta &
175 Chakrabarty, 2013). In the current study, tomato stem was selected as the injection site.

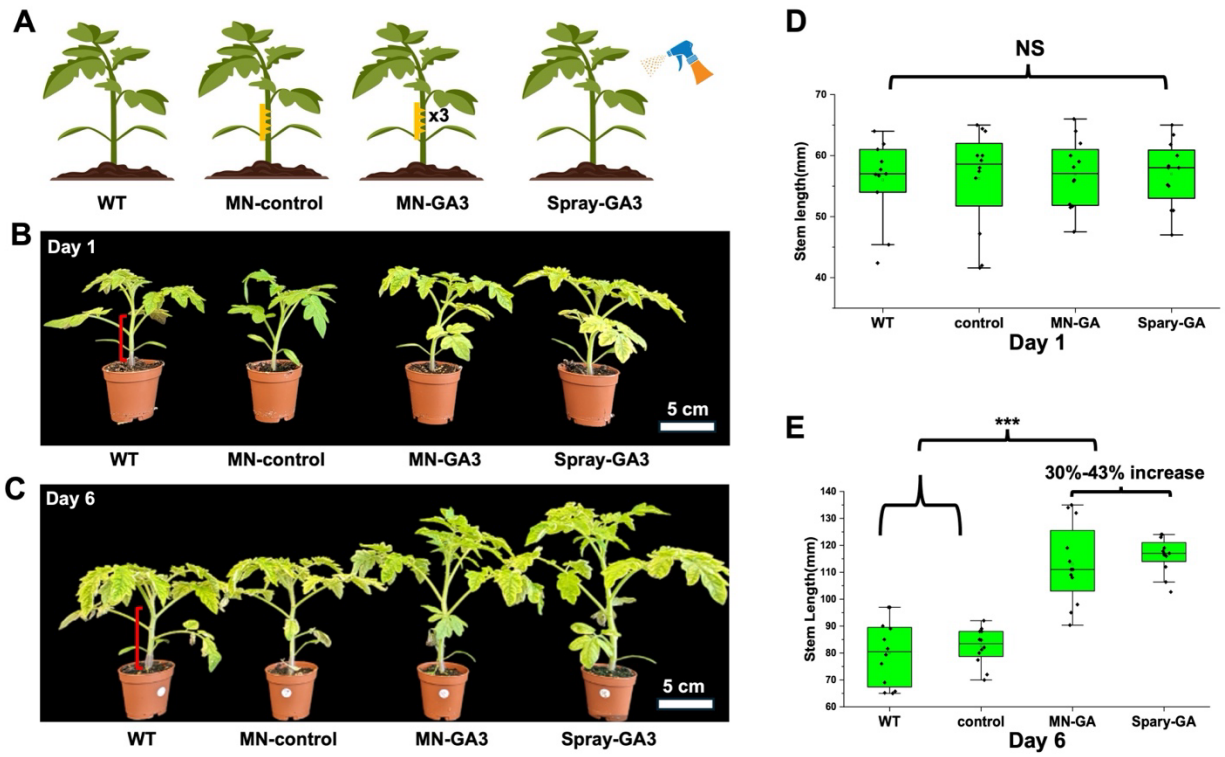

Fig. 2: Tomato phenotype characterization with and without the MN-GA3 (gibberellic acid) treatment. A. Schematic of GA3 treatment model on 25-day-old tomato plants using MN or spray-based delivery methods. **B.** The phenotype of 25-day-old tomato plants after different GA3 treatments. **C.** The phenotype changes of tomato plants (same plants in 2B) 6 days after different GA3 treatments. D. The stem length of the tomato plants at Day 1 after the MN-GA3 and Spray-GA3 treatments (n=12). **E.** The stem length of the tomato plants at Day 6 after the MN-GA3 and Spray-GA3 treatments (n=12).

25-day-old tomato plants (n=12) were injected with the PVA-MN-GA on the stem tissue (Figure 2A, Figure S4). Following the initial MN injection, secondary and tertiary injections were performed 3 and 6 days later, respectively. As controls, plants injected with PVA-MN without GA3 (negative control, or "MN-control") and plants sprayed with GA3 on their leaves (positive control, or "Spray-GA3") were included in the experiment (Figure 2A). In addition, healthy plants without any MN or GA3 treatment were used as the wild type ("WT", Figure 2A). The PVA-MN patch contains 500 μM GA3, which is higher than the loading concentration of GA3 in the spray method (100 μM). However, due to the much smaller delivery volume of the PVA-MN method

193 (only an array of ~ 4 x 10 needles touch stems) compared to 5-10 mL of solutions applied in the
194 spray method, three treatments of PVA-MN deliver an estimated total amount of 0.05-0.075 μmol
195 of GA3, which is only about 10% of the spray method (Table 1).

196 After 6 days, we observed that tomato plants treated with MN-GA3 or Spray-GA3
197 exhibited a faster growth rate compared to control plants (both WT and MN-control, Figure 2B,
198 C). Stem lengths (labeled in red, Figure 2B and 2C) were measured at the same time (Figure 2D),
199 revealing that after 3 days, the heights of MN-GA3 and Spray-GA3-treated tomato plants were
200 18%–21% higher than those of the WT or MN-control plants (Figure S4C). After 6 days, GA3-
201 treated plants showed an increase of 30%–43% in height compared to the non-treated controls
202 (Figure 2E). It is noticed that even though the PVA-MN method achieved similar delivery effect
203 compared to conventional spray method (Figure 2E), it showed slightly larger error bars compared
204 to the traditional leaf-spray methods. This may be due to individual differences in the plant and
205 injection location-induced variations of the PVA-MN delivery system.

206 Additionally, GA3 based PVA-MN injection was also performed on the lateral branch by
207 using 40-day-old tomato plants (Figure S5A and S5B). The injection process is the same with the
208 stem treatment. Due to the difference in the initial length of each lateral branch, we calculated the
209 relative lateral branch elongation to evaluate the GA stimulation. The results showed that after 3
210 days of treatment, the average lateral branch of MN-GA3 and Spray-GA3-treated tomato plants
211 grew around 5% more than the WT and MN-control plants (Figure S5C); After 6 days post-
212 injection, the average lateral branch length increased by nearly 10% of control groups (Figure
213 S5D).

214 In addition to stem or branch growth length difference, we also observed that the tomato
215 plants in GA3-treated groups (MN-GA3 and Spray-GA3) showed a noticeable color difference
216 from 4th to 6th compound leaf (newly emerging leaves) (Figure S6A). We assume that this
217 phenotype difference is probably due to the accelerated growth under the GA3 triggering. The
218 concentration of chlorophyll a ($p = 0.0049$) and b ($p = 0.0025$) in the 4th to 6th leaves (mix samples)
219 was quantified. The results showed that in GA3-treated tomato, the leaf chlorophyll a and b content
220 decreased by 6% to 10% compared to the WT and PVA-MN control plants (Figure S6B and S6C).

221 To investigate whether the MN-GA3 treatment would trigger the intrinsic gene
222 transcription level change in tomato plants. We conducted a series of reverse transcription-

quantitative polymerase chain reaction (RT-qPCR) experiments using tomato leaf samples after different treatments. We selected the GA-signal receptor, two tomato *SID* genes (Shohat *et al.*, 2021), as targets and ran the gene expression analysis. The results revealed that after the MN-GA3 or Spray-GA3 treatments, both *SiSID1* and *SiSID1b1* genes showed significant increases in transcription level by 2 to 15 folds compared to the WT and MN-control plants (Figure 3). The expression level of MN-GA3 group is generally comparable to the Spray-GA3 group (Figure 3). Interestingly, in individual plant #9, the MN treatment promoted a higher level of *SID* gene expression than the conventional spraying. All these above data strongly suggest that the PVA-MN-GA injection promotes the stem or branch growth similarly to the foliar spray method, while reducing the application dose by 10~20 times. Consistently, the gene expression involved in the GA signal in tomato plants was also upregulated, confirming the effectiveness of MN delivery of GA into tomato plants.

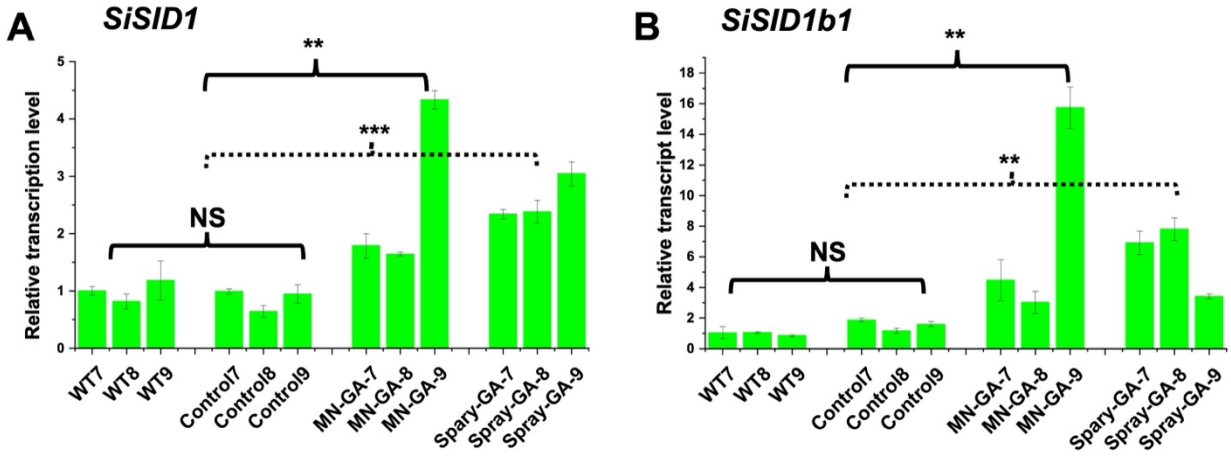

Fig. 3: Tomato gene expression level under different GA stimulations using PVA-MN or GA3 spray. A. The relative transcription level change of *Slsid1* genes under the different GA treatments in tomato plants. Each group has three different plant lines (plants 7, 8, 9). B. The relative transcription level change of *Slsid1b1* genes under the different GA treatments in tomato plants. Each group has three different plant lines (plants 7, 8, 9). (NS: none significant, *P < 0.05, **P < 0.01, ***P < 0.001)

244 **PVA-MN for GA3 Delivery to *Arabidopsis ft-10 mutant***

245 Besides tomatoes, we also used the model plant *Arabidopsis thaliana* and investigated the PVA-
246 MN injection effects on GA signaling process. *Arabidopsis thaliana* showed multiple advantages
247 in phenotyping analysis such as well-characterized biological activities, ease of genetic
248 manipulation, and comprehensive genomic information.

249 Numerous studies have shown that applying gibberellins (such as GA3) in *Arabidopsis*
250 promotes the termination of vegetative growth, inhibits flower formation, accelerates bolting, and
251 results in plants with fewer rosette leaves and more cauline leaves (Bao *et al.*, 2020). Under normal
252 conditions, wild-type *A. thaliana* Col-0 plants produce around 14 rosette leaves during the
253 vegetative growth phase before inflorescence emergence at approximately 23 days under a 16-
254 hour light regime. Some studies report 11–13 rosette leaves between days 21–24 (Cao et al., 2023).
255 Cao and colleagues studied the *Arabidopsis ft-10* mutant, a *FT* gene loss-of-function mutant with
256 a clear late-flowering phenotype under long-day conditions, to evaluate their silk-based
257 microneedle delivery system (Cao et al., 2023). This mutant disrupts non-GA3-related pathways
258 that predominantly regulate flowering under long-day conditions (Figure S7A). Unlike the
259 previous silk-based microneedles, our study applied PVA-MN to the petiole of a single rosette leaf
260 in *Arabidopsis* plants (Figure S7B, C). The PVA-MN used in this experiment was 800 μm in height.

261 To assess the effectiveness of PVA-MN in delivering GA3 to *Arabidopsis* plants, we
262 compared MN-mediated delivery to foliar spray again. Additionally, an empty PVA-MN (without
263 GA3) was used as a negative control (MN-control, Figure 4A). GA3 was delivered via PVA-MN
264 injections at multiple leaves every 3 days, for a total of three applications, similar to the frequency
265 of foliar sprays. For MN injection on *Arabidopsis* vein, a small array of 2x10 needles were used.
266 The spray method used 2~4 mL GA3 solution instead. The total GA3 amount delivered by the
267 spray method is nearly 10 times of that used in the MN injection methods (Table1).

268

269

270

271

272 **Table 1. Comparison of plant hormone consumption in different delivery methods**

Plants	Cargo	Delivery Methods		
		MN-GA	Spray-GA	
Tomato	GA	0.05~0.075 μmol	0.5~1 μmol	
Arabidopsis		0.025~0.03 μmol	0.2~0.4 μmol	
		MN-SA	Spray-SA	Infiltration-SA
Nicotiana Benthamiana	SA	1.2~1.6 μmol	200~250 μmol	50 μmol

273

274 We observed that both Spray-GA and MN-GA treatments resulted in an early bolting
275 phenotype compared to the *ft-10* mutant control and the MN-control (MN only, without GA3)
276 (Figure 4B). Although PVA-MN-GA-treated plants bolted earlier than the controls, their response
277 was slower than that of Spray-GA-treated plants (Figure 4B). Rosette and cauline leaf numbers
278 were also recorded throughout the growth period. GA3-loaded PVA-MN injections produced
279 phenotypes in *ft-10* similar to those observed in GA3 foliar-sprayed plants, with changes in rosette
280 and cauline leaf numbers and leaf size. These phenotypes were significantly different from those
281 *ft-10* mutants untreated with GA3 (Figure 5A). This confirms that GA3 delivered via microneedles
282 effectively altered plant metabolism. Interestingly, MN-control plants (without GA3) produced
283 fewer rosette leaves than the untreated *ft-10* mutant, suggesting that PVA-MN injection may
284 induce some stress even in the absence of GA3 (Figure 5A). These phenotypic findings
285 demonstrate that PVA-MN is effective in delivering GA3 to *Arabidopsis* plants and change their
286 growth behavior accordingly.

287

288

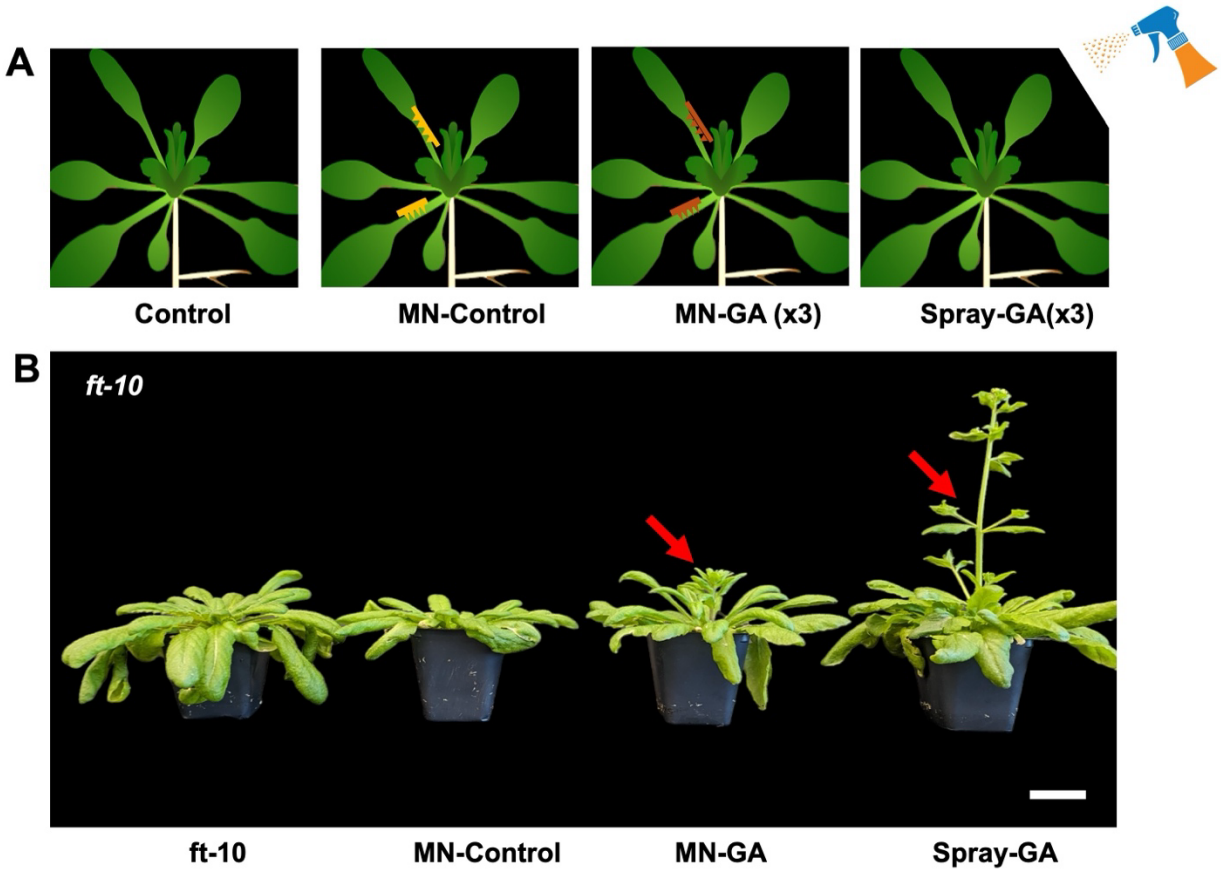

Fig. 4: PVA-MN for GA3 delivery to Arabidopsis ft-10 mutant. A. Schematic of GA3 delivery to Arabidopsis *ft-10* mutant by PVA-MN and spray methods. B. Representative images of ft-10 plants 10 days after different GA treatments. MN injection and spray were carried out every three days. 4 groups of *ft-10* (n=5 for each group) were treated differently (*ft-10*, MN-control, MN-GA3, Spray-GA3).

In *Arabidopsis* plant, there are three GA receptor isoform genes, namely *AtGID1a*, *1b,* and *1c*. Using RT-qPCR, we analyzed the transcript level of these three genes with and without the PVA-MN-GA3 treatment. We detected that the *AtGIA1a* showed a low transcript level in the *Arabidopsis ft-10* mutant background, but the other two GA receptor genes, the *AtGID1b* and *AtGID1c*, showed a significant increase of the mRNA level by 2 to 10 folds after the MN-GA and Spray-GA treatments (Figure 5B). These molecular results confirm the previous phenotypic

observations, suggesting that PVA-MN is an effective tool for delivering plant hormones in *Arabidopsis*.

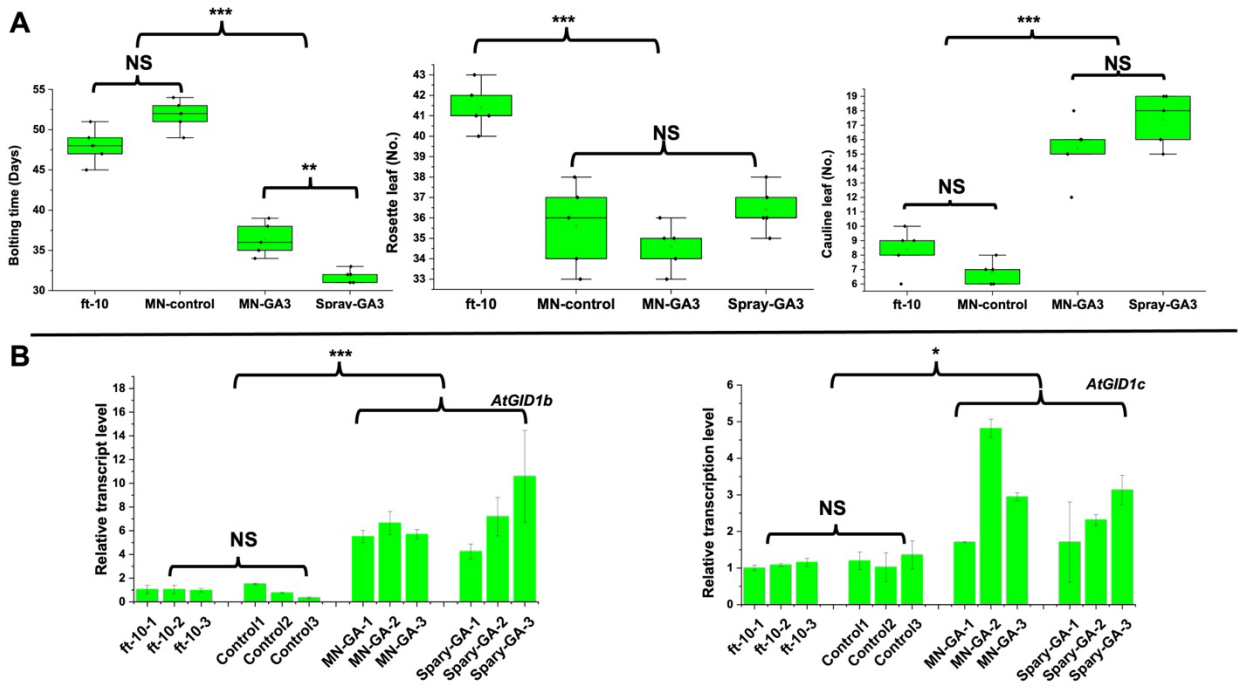

Fig. 5: Different GA delivery treatments change the Arabidopsis phenotype and gene expression in GA signal pathway. A. The bolting time, rosette leaf number, and cauline leaf number change under different GA treatments in Arabidopsis ft-10 mutants. B. The relative transcription level change of *AtGID1b* and *AtGID1c* genes under different GA treatments in tomato plants. Each group has three different plant lines (plants 1, 2, 3). (NS: none significant, *P < 0.05, **P < 0.01, ***P < 0.001)

Delivery of SA for induced TSWV resistance in *Nicotina Benthamiana* plant

The Tomato Spotted Wilt Virus (TSWV) is a plant virus that belongs to the family *Tospoviridae* and is one of the most economically significant plant viruses affecting crops worldwide (Best, 1968). The infected plants often show necrotic spots, wilting, chlorosis (yellowing), stunted growth, leaf deformation phenotype, and in some cases, ring spots or concentric patterns on leaves and fruits. These symptoms lead to reduced yield and poor fruit quality. Plant hormone salicylic

acid (SA) has been shown to help plants to play a significant role in triggering the resistance response to Tomato Spotted Wilt Virus (TSWV) in plants (Turina *et al.*, 2016). SA is a crucial plant hormone involved in systemic acquired resistance (SAR), a defense mechanism that provides broad-spectrum resistance to a variety of pathogens, including viruses like TSWV (Durner *et al.*, 1997). In the following experiment, we used PVA-MN to deliver SA directly into plant tissues and investigated whether the MN microinjection could help the model plant *Nicotiana Benthamiana* generate resistance to the TSWV stress. Normally, the TSWV would move within plants through a well-coordinated process that involves both cell-to-cell movement and systemic movement via the plant's vascular system. To monitor the TSWV movement in the plant, we transformed the gene cassette that encodes a reporter *RUBY* that converts tyrosine to vividly red betalain in viruses (Liu *et al.*, 2023), which makes the viruses directly visible to naked eye after infection on the plant (Figure S8).

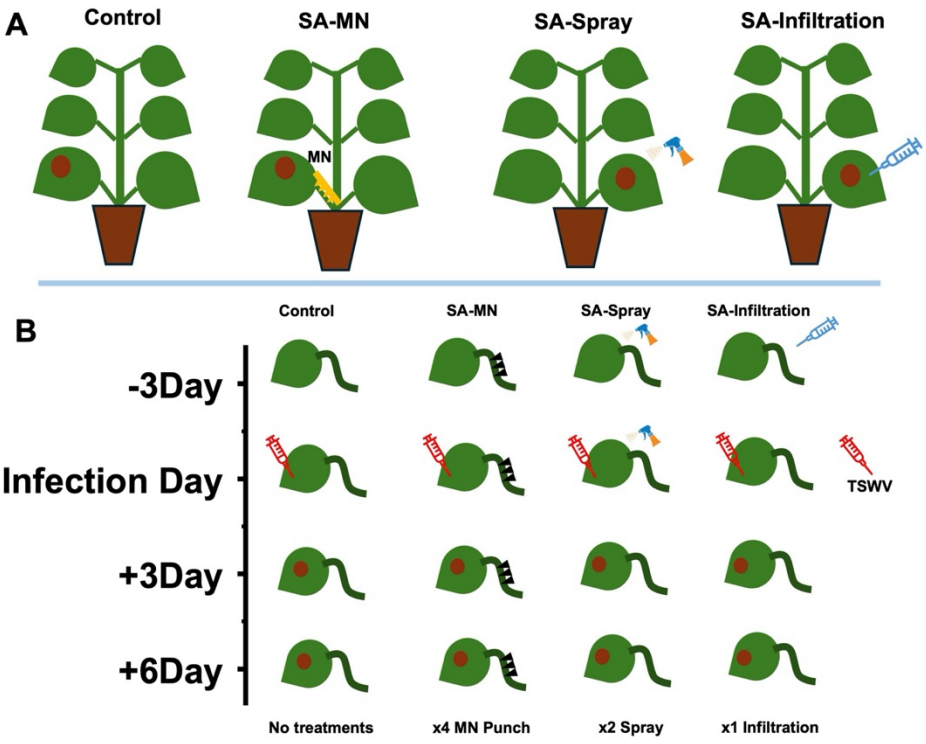

Fig. 6: Schematic showing SA delivery experiments to prevent TSWV virus moving in *Nicotiana Benthamiana* plants. A. A testing model showing different SA delivery approaches. B. A treatment timeline showing the SA treatment process for SA-MN, SA-spray and SA-infiltration on *Nicotiana Benthamiana* plants.

336

337 We compared the SA delivery and treatment efficiency of four different methods, including
338 Control (no SA delivery), SA-MN, SA-Spray, and SA-infiltration (Figure 6A). For SA-MN, the
339 MN patch loaded with SA was applied to tobacco petiole for 4 times in total (1x before and 3x
340 after TSWV inoculation). The SA-Spray method was performed 2 times (before and after
341 inoculation) and SA-Infiltration method was only performed 1 time on *Nicotiana Benthamiana*
342 leaf (Figure 6B). For PVA-MN injection on one tobacco plant, a small MN array of 4x10 needles
343 was used. The spray and infiltration treatments used 20-25 mL and 8-10 mL of SA solutions,
344 respectively. The absolute amounts of SA delivered to tobacco plants by different delivery
345 methods are summarized in Table 1.

346 All treatments started on 20-day-old *Nicotiana Benthamiana* plants three days before
347 inoculation. Then, on Day 0, the TSWV-RUBY was transformed into a plant via the infiltration
348 method. In the meantime, the SA-MN and SA-Spray treatments were conducted for the second
349 round. The third and fourth SA-MN punch treatments were performed 3 and 6 days later after
350 TSWV infection (Figure 6B).

351 In the first trial, the SA-MN group applied 2 mM SA, while the SA-Spray and SA-
352 Infiltration groups used only 500 uM SA, given their larger application volumes. Still, the
353 estimated amount of SA delivered to the plants by the MN approach is only about 0.5-1% of the
354 spray or infiltration method (Table 1). Once TSWV-RUBY is infected, the infection site on the
355 leaf develops light-to-dark red colors, accompanied with the virus progression. 3 days after
356 inoculation, we observed the virus infection in all test groups and found that near 67% of the
357 infected leaves on Control plants (without SA treatment) turned dark red color. However, only
358 about 20% of the leaves showed dark color in SA-treated plants (Figure 7A, no major differences
359 between SA-MN, SA-Spray, and MN-infiltration). After 6 days, nearly 92% of the infected leaves
360 were dark red in the Control plants. At the same time, the percentage of dark red color in SA-
361 treated groups was kept lower at around 50% (Figure 7A). These results suggest that the SA
362 treatment would inhibit TSWV infection.

363 This indicates MN is a highly effective delivery platform for sending SA into leaf tissues
364 and inducing TSWV resistance. It is also interesting to note that after 15 days of viral infection,
365 all the infected leaves demonstrated a dark red color and died due to virus infection. The petioles

366 of Control, SA-Spray and SA-infiltration groups all turned red color (Figure 7B), indicating the
367 transportation of TSWV along the plant vasculature system. However, the SA-MN treated petiole
368 remained green (Figure 7B), indicating a strong viral resistance and fewer viral transportation in
369 the SA-MN treated petiole tissue.

370 The comparison experiments were repeated by increasing the concentration of SA in SA-
371 Spray and SA-infiltration methods to 1 mM instead of 500 μM (Figure S9A). After 20 days of
372 infection, the Control group clearly showed that the movement of TSWV from the leaf tissue to
373 the stem, along the vein in the WT *Nicotiana Benthamiana* plants (Figure S9B). However, in SA-
374 MN, SA-Spray, and SA-infiltrated plants, no red color on the stem was observed (Figure S9B).
375 After 30 days of infection, the Control plant revealed a dwarf phenotype compared to the SA-
376 treated plants (Figure S10A). The stem of Control plants showed tissue wilting. On the contrary,
377 the SA-MN and SA-Spray treated plants were still healthy, while few red color was also found in
378 SA-infiltrated plants (Figure S10B), which may be due to less total SA treatment dose in the
379 infiltration method (infiltration: 5 mL of 1 mM SA; Spray: 10 mL of 1 mM SA and repeated 2x).

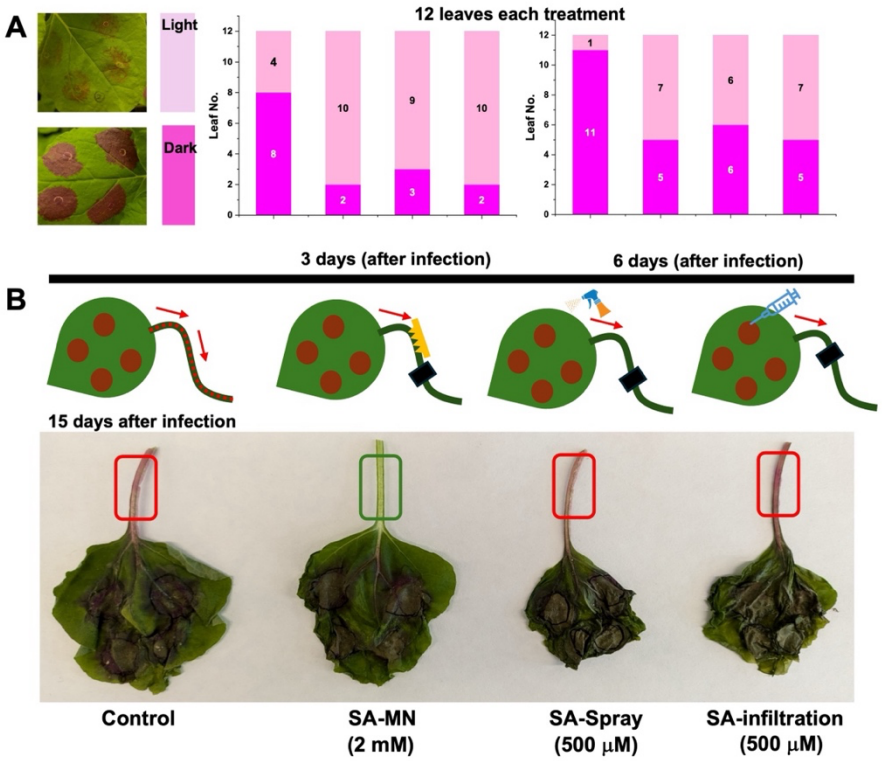

380

381 **Fig. 7: SA-MN delivery prevents TSWV development and movement on the *Nicotiana***
382 ***Benthamiana* leaf**. A. The color change of red TSWV (RUBY as a reporter) after infection on

383 *Nicotiana Benthamiana* leaf under the SA treatments at 3 days and 6 days, respectively. The light
384 red color indicated the early stage of TSWV infection, while the dark red color indicated the deep
385 infection degree. B. Th phenotype of TSWV infected-*Nicotiana Benthamiana* (15 days post
386 infection). SA-MN delivery inhibited the TSWV movement from the leaf to petiole.

387 These experiments strongly suggested that the SA could be effectively delivered to
388 *Nicotiana Benthamiana* plants by the MN delivery method and induce resistance to TSWV
389 infection. Compared to the traditional spray method, although the SA-MN method is more frequent
390 (total four times) and has a higher SA concentration (2 mM), it significantly reduces the total
391 application dose by ~99% (Table 1) while achieving similar immunization effects. Moreover, the
392 spray method required multiple treatment positions, including the applications to adaxial and the
393 abaxial sides of the leaf, while the PVA-MN injection simply works on the stem or petiole. This
394 suggests that our PVA-MN delivery method is more economical, convenient, and efficient.

395 **Discussion**

396 In this study, we demonstrated that PVA MN patches could be effectively utilized as a precision
397 plant delivery system for various compounds, including small-molecule dyes, growth hormones,
398 and antiviral agents (Figure 8). Compared to conventional delivery methods such as foliar spray
399 and soil application, which suffer from high chemical losses, environmental impact, and low
400 absorption, PVA-MNs offer a promising alternative that can directly target plant tissues with high
401 precision and reduced application dose and environmental side effects. Our results showed that the
402 PVA-MNs successfully delivered fluorescent dyes into the vascular tissues of tomato stems,
403 confirming the capability of these MNs to penetrate plant tissues and facilitate compound diffusion.
404 This is significant as it highlights the unique advantage of PVA-MNs to enhance the uptake and
405 transport of bioactive molecules within plants, addressing a critical limitation of foliar and soil
406 applications, where the efficacy of nutrient and agrochemical delivery is compromised by
407 environmental factors and the natural barriers of plant surfaces.

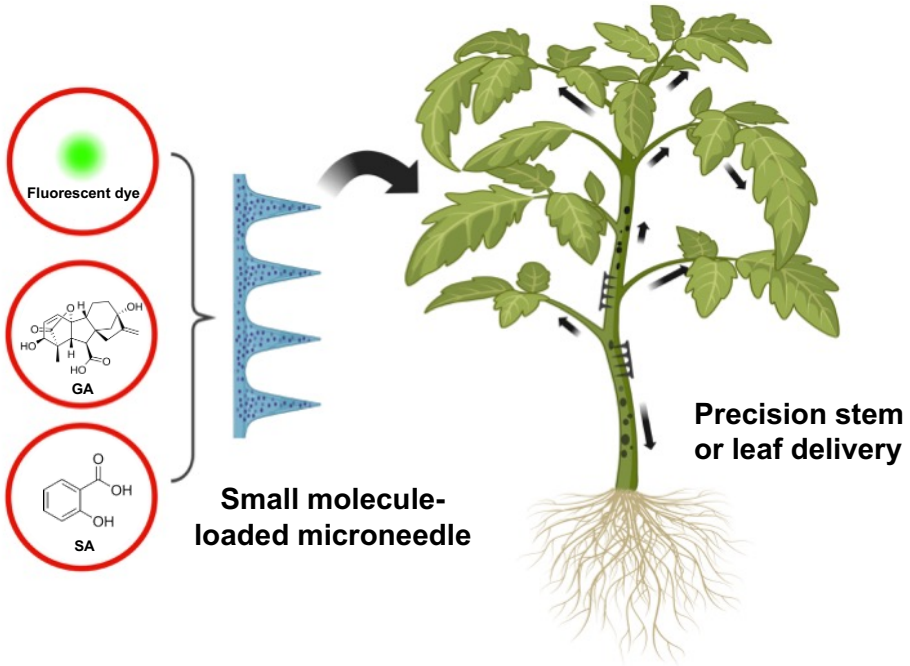

Fig. 8: Schematic of PVA microneedle delivery platform for delivering different cargos into a live plant.

The delivery of GA3 through PVA-MNs in tomato plants resulted in accelerated stem growth and an altered chlorophyll profile in newly emerged leaves, indicating effective hormone delivery and physiological response. Compared to traditional foliar spray methods, MNs demonstrated similar or slightly enhanced growth-promoting effects while reducing application amount of GA3 by nearly 90%, suggesting that PVA-MNs is a more controlled and sustained delivery method. The transcriptional upregulation of GA receptor genes further supports the successful delivery of GA3, confirming that MNs can effectively trigger hormonal signaling pathways in planta. In *Arabidopsis ft-10* mutants, known for their delayed flowering phenotype, PVA-MN-mediated GA3 delivery induced earlier bolting, resembling the phenotypic response seen with foliar sprays. This response validates the use of MNs for delivering hormones in a model plant system and emphasizes their potential utility in precision agriculture to manipulate plant growth and development. The observed upregulation of GA receptor genes in treated plants

underscores the ability of PVA-MNs to modulate gene expression and drive desired phenotypic outcomes.

Finally, the application of SA via PVA-MNs in *Nicotiana Benthamiana* demonstrated the MN's ability to enhance plant resistance against TSWV, a new way of plant immunization with high accuracy. The restricted movement of the virus in SA-treated plants highlights the effectiveness of MNs in delivering antiviral compounds directly to the infection site, enhancing the plant's natural defense mechanisms. This approach offers a targeted method to combat viral infections, potentially reducing the need for broad-spectrum chemical treatments that can harm the environment.

Despite these promising results, several challenges remain to in implementing MN-based delivery methods in future. For instance, the dehydration effect observed in MN-treated leaf tissues suggests that MN application may be more suitable for stems or thicker plant parts where the tissue is more robust. Stem delivery may potentially also accept a larger amount of payloads and transport the delivered payloads faster to other parts of the plant than leaf delivery. Additionally, while MNs provide a more direct and potentially more efficient delivery option, the injection process could be further automated in future (e.g., use of robotic arms) to scale up the process and minimize tissue damage by more controlled pressure application.

Overall, our findings suggest that PVA-MNs are a viable and effective tool for plant compound delivery, offering benefits over traditional methods in terms of precision, efficiency, and reduced environmental impact. Future research should focus on scaling up MN fabrication processes, automating delivery techniques, and expanding the range of compounds that can be effectively delivered through this innovative system. With continued development, MN delivery technology could potentially revolutionize precision agriculture, enabling more sustainable and targeted interventions in crop management.

Materials and methods:

Plant materials and growing conditions

451 Arabidopsis thaliana ft-10 mutant seeds (TAIR Germplasm CS9869) and ecotype Columbia (Col-
452 0) seeds were sterilized by soaking for 1 min in 70% ethanol and then for 10 min in 20% bleach,
453 followed by five to seven rinsing with sterile distilled water. Sterilized seeds were placed on
454 Murashige and Skoog (MS) plates and kept at 4 °C for 2 days. The plate was placed in a plant
455 growth chamber (Caron 7304-22-1) at 22 °C with long day (day/night 16h/8h) conditions, 70–100%
456 relative humidity, and light intensity of 100 μmol m^{-2} s^{-1}. Seedlings were transferred to pots (2.5
457 × 2.5 × 3 in^3) with soil (Miracle-Gro Moisture Control Potting Soil Mix) on day 7 and watered
458 regularly. Tomato (Solanum lycopersicum var. Beefsteak) seeds were purchased from The Seed
459 Plant. Tomato and lettuce seeds were grown in pots (3.5 × 3.5 × 3 in^3) in the plant room under
460 long day (day/night 16h/8h) at 80 μmol m^{-2} s^{-1}, 70–90% relative humidity, day and night
461 temperatures of 26 and 20 °C, respectively. *Nicotiana Benthamiana* plants were grown in the
462 growth chamber at 12h day and 12h night at 26°C at 275 μmol m^{-2} s^{-1}.

463 **TSWV virus infection**

464 *Agrobacterium tumefaciens* GV3101 carrying recombinant plasmids (pL, pM-RUBY, pS-NSs,
465 and triple VSR (viral suppressor of RNAi) were grown in Luria Broth media containing
466 appropriate antibiotics (Rifampicin (50 μg/ml), Kanamycin (50 μg/ml), and Gentamycin
467 (50 μg/ml)) for overnight. Cells were harvested from overnight grown cultures of *Agrobacterium*
468 and re-suspended into the infiltration buffer (10 mM $MgCl_2$, 10 mM MES pH 5.6 and 100 μM
469 acetosyringone) at OD600 of 1, and further incubated at 28ºC for 3 hours. Before infiltration,
470 *Agrobacterium* cultures carrying pL, pM-RUBY, pS-NSs, and triple VSR plasmids were mixed at
471 final OD600 of 0.25. Three hours post-incubation, fully expanded *Nicotiana benthamiana* leaves
472 were co-infiltrated with *Agrobacterium* cells harboring pL, pM-RUBY, pS-NSs, and triple VSR
473 plasmids at final OD600 of 0.25 (Liu et al., 2023).

474 **PVA MN fabrication process**

475 The microneedle patch was fabricated using a simple centrifugation method using
476 polydimethylsiloxanes (PDMS)-based negative molds (Blueacre Technology) in a 10 (w/v) %
477 polyvinyl alcohol (PVA) (M.W. 31,000-50,000, 98.0-98.8% hydrolyzed) (Acros Organics)
478 solution. To remove dust and debris from the micron-scale crevices of the PDMS molds, each chip
479 is first cleaned by repeated rinses with deionized (DI) water followed by two rounds of sonication

480 for 5 minutes each. The molds then dried at 35°C for 10-20 minutes to evaporate any remaining
481 water droplets clinging onto the needle edges. Next, 1.2 mL of PVA is allotted in 1.7 mL centrifuge
482 tubes which undergo their first round of centrifugation at 7500 rpm (Fisher Scientific accuSpin
483 Micro17) for 10 minutes without the mold to remove any trapped air bubbles. The molds are then
484 submerged into these tubes with the needle molds facing inwards and centrifuged again at 7500
485 rpm for 10 minutes to facilitate PVA flow into the holes. The molds are then removed and sealed
486 with another layer of PVA to allow the formation of a stronger base for the needles upon drying.
487 Lastly, the MN patches are partially covered (for slow evaporation) and cured for 24 hours at room
488 temperature to allow complete solidification.

489 *MN patch fabrication with Gibberellic acid (GA3):* 34.6 mg of GA3 is dissolved in 500 µL
490 of dimethylsulfoxide (DMSO) and 500 µL of deionized (DI) water to make a stock solution of 100
491 mM of GA3. 6 µL of the solution is added to 1.2 mL of 10 (w/v) % PVA solution to make a final
492 GA3 concentration of 500 µM in 10 (w/v) % PVA solution for one microneedle patch. Each 20 x
493 20 MN array is made from 500 µL PVA-GA3 solution. In the tomato treatment experiments, only
494 a 4 x 10 array was pressed to the plant stem due to the small size of plant stems. The estimated
495 amounts of total GA3 delivered to different plants by MN are summarized in Table 1.

496 *MN patch fabrication with Salicylic Acid (SA):* 11.04 mg of SA is dissolved in 15 mL of
497 DI water to make a stock solution of 5.33 mM. This solution is then added to 16 (w/v) % PVA
498 solution to make a final solution of 2 mM SA and 10% (w/v) PVA for microneedle fabrication.

499 *MN patch fabrication with Rhodamine and 5(6)-carboxyfluorescein (5(6)-FAM):* 52 mg of
500 Rhodamine is dissolved in 1.2 mL DI water to make a stock solution of 0.0905 M. On the other
501 hand, to make a stock solution of 0.2715 M 5(6)-FAM, 25 mg of the powder is dissolved in 200
502 µL of DMSO. 33 µL and 11 µL of the respective stock solutions were added to 30 mL of 10 (w/v) %
503 PVA to make a final solution containing 0.1 mM of Rhodamine and 5(6)-FAM each that was used
504 to fabricate the microneedles.

505 **Fluorescent dye delivery in tomato plants**

506 5(6)-carboxyfluorescein diacetate (1 mM) and rhodamine 6G (1 mM) were mixed with a DMSO
507 solution at a volume ratio of 1:100 when fabricating the PVA-MN. To monitor fluorescence signal
508 from the delivery and transport of 5(6)-carboxyfluorescein diacetate and rhodamine 6G, cross-

509 sections upstream and downstream along the petiole were observed under a microscope with fixed
510 light intensity and an exposure time of 20 ms. The petiole was also sliced longitudinally to image
511 the distribution profile of 5(6)-carboxyfluorescein diacetate in the xylem. Image analysis was
512 performed using ImageJ 1.52i. Fluorescence intensity was used as a proxy for the concentration of
513 5(6)-carboxyfluorescein diacetate within the tested range, and fluorescence signals were integrated
514 radially.

515 **Plant hormone preparation**

516 GA3 Solution Preparation: 0.1 M stock solution of GA3 was prepared by dissolving 34.6 mg GA3
517 in 1 mL 75% ethanol solution. GA3 spray solution was prepared by diluting stock solution 1000×
518 to a final concentration of 100μM. Silwet-77 was added to obtain a final concentration of 0.01%
519 in the GA3 spray.

520 SA Solution Preparation: 100 mM stock solution of SA was prepared by dissolving 138
521 mg SA in 1 mL 75% ethanol solution. The SA spray solution was prepared by diluting 100 mM
522 SA stock 1000X to the final concentration of $0.1x10^{-3}$ M. Tween-20 was added to obtain a final
523 concentration of 0.01% in the SA spray and used as a surfactant to promote SA absorption.

524

525 **QRT-PCR based gene expression analysis**

526 Quantitative RT-PCR analysis was performed using SYBR-Green PCR Master mix (Invitrogen,
527 Carlsbad, CA, United States) on a CFX96TM (Bio-Rad, California, CA, United States). Gene-
528 specific primer pairs and different thermal programs (Supplementary Table S1) were developed to
529 compare expression levels in *Arabidopsis*, tomato, and *Nicotiana Benthamiana* plants.
530 Arabidopsis *UBQ10* gene and tomato Actin gene were used as reference controls for normalization.
531 Amplified products were monitored using an optical reaction module (SYBR-green) and the
532 resulting amplified values of genes were normalized against those of references according to a
533 previous protocol for plants (Li *et al.*, 2021). Steps of PCR analysis were carried out following the
534 method described previously (Li et al., 2021). The reaction system was composed of 12 μL mixture,
535 including: 10 μL of SYBR-green-preMix, 1.0 μL of 10 μM forward and reverse primer, and 1.0
536 μL of cDNA template(Li *et al.*, 2017). The thermal program followed the protocol of Bio-rad
537 SYBR-Green PCR Master-mix. The thermal program is 95 ºC for 30s, (95 ºC for 10s, 60 ºC for 1

538 min) ×40, 65 ºC to 95 ºC with 0.5 ºC increments in 2s, 4 ºC. Three replicates were performed in
539 this assay for each gene expression analysis. All the primers were listed in Supplementary Table
540 S1.

541 **Funding:** The authors sincerely thank the funding support provided by Kenan Institute and the
542 Game-Changing Research Incentive Program for the Plant Sciences Initiative (GRIP4PSI).

543 **Author Contribution:**

544 M.L. contributed to experiment design, plant treatments, RNA extraction, analysis of all
545 experimental data, figure preparation, and manuscript drafting. A.D.P. contributed to PVA-MN
546 preparation. D. S. and A. W. helped constructed the RUBY-TSWV and TSWV infection
547 experiments. Q.W. perceived and designed the project, developed experimental plans, supervised
548 data analysis and figure preparation. All authors contributed to the revision of the manuscript.

549 **Acknowledgements:**

550 The authors thank Dr. Hongwei Jing and Dr. Wusheng Liu at NC State Department of Horticulture
551 for helping with RNA extraction.

552 **Declaration of interests:**

553 The authors declare that the research was conducted in the absence of any commercial or financial
554 relationships that could be construed as a potential conflict of interest.

555

556

557

558

Reference:

Alkharabsheh, H. M., Seleiman, M. F., Battaglia, M. L., Shami, A., Jalal, R. S., Alhammad, B. A.*, et al.* (2021) Biochar and its broad impacts in soil quality and fertility, nutrient leaching and crop productivity: A review. *Agronomy,* **11,** 993.

Bao, S., Hua, C., Shen, L. and Yu, H. (2020) New insights into gibberellin signaling in regulating flowering in Arabidopsis. *Journal of Integrative Plant Biology,* **62,** 118-131.

Barłóg, P., Grzebisz, W. and Łukowiak, R. (2022) Fertilizers and fertilization strategies mitigating soil factors constraining efficiency of nitrogen in plant production. *Plants,* **11,** 1855.

Beig, B., Niazi, M. B. K., Sher, F., Jahan, Z., Malik, U. S., Khan, M. D.*, et al.* (2022) Nanotechnology-based controlled release of sustainable fertilizers. A review. *Environmental Chemistry Letters,* **20,** 2709-2726.

Best, R. J. (1968) Tomato spotted wilt virus. *Advances in virus research,* **13,** 65-146.

Brichi, L., Fernandes, J. V., Silva, B. M., Vizú, J. d. F., Junior, J. N. and Cherubin, M. R. (2023) Organic residues and their impact on soil health, crop production and sustainable agriculture: A review including bibliographic analysis. *Soil Use and Management,* **39,** 686-706.

Cao, Y., Koh, S. S., Han, Y., Tan, J. J., Kim, D., Chua, N. H.*, et al.* (2023) Drug delivery in plants using silk microneedles. *Advanced Materials,* **35,** 2205794.

Cao, Y., Lim, E., Xu, M., Weng, J. K. and Marelli, B. (2020) Precision delivery of multiscale payloads to tissue-specific targets in plants. *Advanced Science,* **7,** 1903551.

Cunningham, F. J., Goh, N. S., Demirer, G. S., Matos, J. L. and Landry, M. P. (2018) Nanoparticle-mediated delivery towards advancing plant genetic engineering. *Trends in biotechnology,* **36,** 882-897.

Davis, K. F., Gephart, J. A., Emery, K. A., Leach, A. M., Galloway, J. N. and D'Odorico, P. (2016) Meeting future food demand with current agricultural resources. *Global Environmental Change,* **39,** 125-132.

Dimkpa, C. O., Fugice, J., Singh, U. and Lewis, T. D. (2020) Development of fertilizers for enhanced nitrogen use efficiency–Trends and perspectives. *Science of the Total Environment,* **731,** 139113.

Durner, J., Shah, J. and Klessig, D. F. (1997) Salicylic acid and disease resistance in plants. *Trends in plant Science,* **2,** 266-274.

Ece, E., Eş, I. and Inci, F. (2023) Microneedle technology as a new standpoint in agriculture: Treatment and sensing. *Materials Today*.

Faraji Rad, Z. (2023) Microneedle technologies for food and crop health: recent advances and future perspectives. *Advanced Engineering Materials,* **25,** 2201194.

Fukase, E. and Martin, W. (2020) Economic growth, convergence, and world food demand and supply. *World Development,* **132,** 104954.

Gupta, R. and Chakrabarty, S. (2013) Gibberellic acid in plant: still a mystery unresolved. *Plant signaling & behavior,* **8,** e25504.

Han, Y., Jangir, M., Ngoh, A. S. Y., Li, C., Sarangapani, S., Cao, Y.*, et al.* (2025) Precise Delivery of Physiological Doses of Melatonin in Planta to Control Postharvest Physiology and Extend Shelf Life Outside the Cold Chain. *Nano Letters*.

602 Ishfaq, M., Kiran, A., ur Rehman, H., Farooq, M., Ijaz, N. H., Nadeem, F.*, et al.* (2022) Foliar
603 nutrition: Potential and challenges under multifaceted agriculture. *Environmental*
604 *and Experimental Botany,* **200,** 104909.
605 Jakhar, A. M., Aziz, I., Kaleri, A. R., Hasnain, M., Haider, G., Ma, J.*, et al.* (2022) Nano-
606 fertilizers: A sustainable technology for improving crop nutrition and food security.
607 *NanoImpact,* **27,** 100411.
608 Jung, J. H. and Jin, S. G. (2021) Microneedle for transdermal drug delivery: current trends
609 and fabrication. *Journal of pharmaceutical investigation***,** 1-15.
610 Krishnasree, R., Raj, S. K. and Chacko, S. R. (2021) Foliar nutrition in vegetables: A review.
611 *Journal of Pharmacognosy and Phytochemistry,* **10,** 2393-2398.
612 Li, M., Dey, P. A., Cui, Q., Hsieh, T.-F., Summeetha, J., Xu, J.*, et al.* (2025) **Non-destructive**
613 **seed genotyping via microneedle-basedDNA extraction**. *Plant Biotecnology*
614 *Journal*.
615 Li, M., He, X., La Hovary, C., Zhu, Y., Dong, Y., Liu, S.*, et al.* (2021) A De Novo regulation
616 design shows an effectiveness in altering plant secondary metabolism. *Journal of*
617 *Advanced Research*.
618 Li, M., Li, Y., Guo, L., Gong, N., Pang, Y., Jiang, W.*, et al.* (2017) Functional characterization
619 of tea (Camellia sinensis) MYB4a transcription factor using an integrative approach.
620 *Frontiers in Plant Science,* **8,** 943.
621 Liu, C., Zhou, H. and Zhou, J. (2021) The applications of nanotechnology in crop
622 production. *Molecules,* **26,** 7070.
623 Liu, Q., Zhao, C., Sun, K., Deng, Y. and Li, Z. (2023) Engineered biocontainable RNA virus
624 vectors for non-transgenic genome editing across crop species and genotypes.
625 *Molecular Plant,* **16,** 616-631.
626 Nagarkar, R., Singh, M., Nguyen, H. X. and Jonnalagadda, S. (2020) A review of recent
627 advances in microneedle technology for transdermal drug delivery. *Journal of Drug*
628 *Delivery Science and Technology,* **59,** 101923.
629 Nair, R., Varghese, S. H., Nair, B. G., Maekawa, T., Yoshida, Y. and Kumar, D. S. (2010)
630 Nanoparticulate material delivery to plants. *Plant science,* **179,** 154-163.
631 Niu, J., Liu, C., Huang, M., Liu, K. and Yan, D. (2021) Effects of foliar fertilization: a review of
632 current status and future perspectives. *Journal of Soil Science and Plant Nutrition,*
633 **21,** 104-118.
634 Nkebiwe, P. M., Weinmann, M., Bar-Tal, A. and Müller, T. (2016) Fertilizer placement to
635 improve crop nutrient acquisition and yield: A review and meta-analysis. *Field crops*
636 *research,* **196,** 389-401.
637 Pahalvi, H. N., Rafiya, L., Rashid, S., Nisar, B. and Kamili, A. N. (2021) Chemical fertilizers
638 and their impact on soil health. *Microbiota and Biofertilizers, Vol 2: Ecofriendly tools*
639 *for reclamation of degraded soil environs***,** 1-20.
640 Paul, R., Ostermann, E., Chen, Y., Saville, A. C., Yang, Y., Gu, Z.*, et al.* (2021) Integrated
641 microneedle-smartphone nucleic acid amplification platform for in-field diagnosis
642 of plant diseases. *Biosensors and Bioelectronics,* **187,** 113312.
643 Paul, R., Ostermann, E. and Wei, Q. (2020) Advances in point-of-care nucleic acid
644 extraction technologies for rapid diagnosis of human and plant diseases.
645 *Biosensors and Bioelectronics,* **169,** 112592.

Paul, R., Ostermann, E. and Wei, Q. (2022) Rapid Extraction of Plant Nucleic Acids by Microneedle Patch for In-Field Detection of Plant Pathogens. In: *Plant Pathology: Method and Protocols*. Springer, pp. 77-90.

Salama, D. M., Abd El-Aziz, M., Rizk, F. A. and Abd Elwahed, M. (2021) Applications of nanotechnology on vegetable crops. *Chemosphere,* **266,** 129026.

Shohat, H., Eliaz, N. I. and Weiss, D. (2021) Gibberellin in tomato: Metabolism, signaling and role in drought responses. *Molecular Horticulture,* **1,** 15.

Sinha, E., Calvin, K. V., Kyle, P. G., Hejazi, M. I., Waldhoff, S. T., Huang, M.*, et al.* (2022) Implication of imposing fertilizer limitations on energy, agriculture, and land systems. *Journal of environmental management,* **305,** 114391.

Tudi, M., Daniel Ruan, H., Wang, L., Lyu, J., Sadler, R., Connell, D.*, et al.* (2021) Agriculture development, pesticide application and its impact on the environment. *International journal of environmental research and public health,* **18,** 1112.

Turina, M., Kormelink, R. and Resende, R. O. (2016) Resistance to tospoviruses in vegetable crops: epidemiological and molecular aspects. *Annual review of phytopathology,* **54,** 347-371.

Tyagi, J., Ahmad, S. and Malik, M. (2022) Nitrogenous fertilizers: Impact on environment sustainability, mitigation strategies, and challenges. *International Journal of Environmental Science and Technology,* **19,** 11649-11672.

Vasundhara, D. and Chhabra, V. (2021) Foliar nutrition in cereals: A review. *Pharma Innov J,* **10,** 1247-1254.

Wang, J. W., Cunningham, F. J., Goh, N. S., Boozarpour, N. N., Pham, M. and Landry, M. P. (2021) Nanoparticles for protein delivery in planta. *Current opinion in plant biology,* **60,** 102052.

Yahaya, S. M., Mahmud, A. A., Abdullahi, M. and Haruna, A. (2023) Recent advances in the chemistry of nitrogen, phosphorus and potassium as fertilizers in soil: a review. *Pedosphere,* **33,** 385-406.

Young, M. D., Ros, G. H. and de Vries, W. (2021) Impacts of agronomic measures on crop, soil, and environmental indicators: A review and synthesis of meta-analysis. *Agriculture, Ecosystems & Environment,* **319,** 107551.

Zhang, H., Cao, Y., Xu, D., Goh, N. S., Demirer, G. S., Cestellos-Blanco, S.*, et al.* (2021) Gold-nanocluster-mediated delivery of siRNA to intact plant cells for efficient gene knockdown. *Nano letters,* **21,** 5859-5866.

Zhang, H., Goh, N. S., Wang, J. W., Pinals, R. L., González-Grandío, E., Demirer, G. S.*, et al.* (2022) Nanoparticle cellular internalization is not required for RNA delivery to mature plant leaves. *Nature nanotechnology,* **17,** 197-205.

Zhang, H., Zhang, H., Demirer, G. S., González-Grandío, E., Fan, C. and Landry, M. P. (2020) Engineering DNA nanostructures for siRNA delivery in plants. *Nature protocols,* **15,** 3064-3087.

Zheng, L., Chen, H., Wang, Y., Mao, Q., Zheng, M., Su, Y.*, et al.* (2020) Responses of soil microbial resource limitation to multiple fertilization strategies. *Soil and Tillage Research,* **196,** 104474.